Benzyl isothiocyanate–induced apoptosis in human breast cancer cells is initiated by reactive oxygen species and regulated by Bax and Bak

Dong Xiao, Victor Vogel, and Shivendra V. Singh

Department of Pharmacology and University of Pittsburgh Cancer Institute, University of Pittsburgh School of Medicine, Pittsburgh, Pennsylvania

Abstract

Epidemiologic studies have revealed an inverse correlation between dietary intake of cruciferous vegetables and the risk of breast cancer. We now show that cruciferous vegetable constituent benzyl isothiocyanate (BITC) effectively suppresses growth of cultured human breast cancer cells (MDA-MB-231 and MCF-7) by causing G_2-M phase cell cycle arrest and apoptosis induction. On the other hand, a normal mammary epithelial cell line (MCF-10A) is significantly more resistant to growth arrest and apoptosis by BITC compared with breast cancer cells. The BITC-mediated cell cycle arrest was associated with a decrease in levels of proteins involved in regulation of G_2-M transition, including cyclin B1, cyclin-dependent kinase 1, and cell division cycle 25C. The BITC-induced apoptosis correlated with induction of proapoptotic proteins Bax (MCF-7) and Bak (MDA-MB-231 and MCF-7) and down-regulation of antiapoptotic proteins Bcl-2 and Bcl-xL (MDA-MB-231). The SV40-immortalized mouse embryonic fibroblasts derived from Bax and Bak double knockout mice were significantly more resistant to BITC-induced DNA fragmentation compared with wild-type mouse embryonic fibroblasts. The BITC treatment caused rapid disruption of the mitochondrial membrane potential, leading to cytosolic release of apoptogenic molecules, which was accompanied by formation of autophagosome-like structures as revealed by transmission electron microscopy. The BITC-mediated apoptosis was associated with generation of reactive oxygen species and cleavage of caspase-9, caspase-8, and caspase-3. Apoptosis induction by BITC was significantly attenuated in the presence of a combined superoxide dismutase and catalase mimetic EUK134 as well as caspase inhibitors. In conclusion, the present study reveals a complex signaling leading to growth arrest and apoptosis induction by BITC. [Mol Cancer Ther 2006;5(11):2931–45]

Introduction

Epidemiologic studies continue to support the premise that dietary intake of cruciferous vegetables may be protective against the risk of various types of malignancies (1, 2). Anticarcinogenic effect of cruciferous vegetables is attributed to isothiocyanates (ITC) that occur naturally as glucosinolates in a variety of edible cruciferous vegetables, including broccoli, mustard, horseradish, watercress, and cabbage (3). Organic ITCs are generated due to hydrolysis of corresponding glucosinolates through catalytic mediation of myrosinase, which is released on damage of the plant cells during cutting or chewing of cruciferous vegetables. Benzyl ITC (BITC) is one of the best studied members of the ITC family of compounds that has attracted a great deal of research interest because of its ability to inhibit chemically induced cancer in animal models (reviewed in refs. 3, 4). For example, BITC is a potent inhibitor of rat mammary and mouse lung carcinogenesis induced by polycyclic hydrocarbons 7,12-dimethylbenz(*a*)anthracene and benzo(*a*)pyrene and hepatocarcinogenesis in rats induced by diethylnitrosamine (5–9). Inhibition of benzo(*a*)pyrene-induced lung tumorigenesis in A/J mice by dietary *N*-acetylcysteine conjugate of BITC has also been documented (10). Impaired carcinogen activation due to inhibition of cytochrome *P*450-dependent monooxygenases and/or enhanced detoxification of the carcinogenic intermediates due to induction of phase 2 enzymes (e.g., glutathione transferases) is believed to be responsible for BITC-mediated inhibition of chemically induced cancers in animal models (3, 4).

In addition to prevention of chemically induced cancers, BITC has been shown to suppress proliferation of cancer cells in culture by causing cell cycle arrest and/or apoptosis induction (11–19). Previous studies have offered novel insights into the mechanism of cell cycle arrest and apoptosis induction by BITC (11–17). However, a review of the published literature also suggests that the mechanism by which BITC causes growth arrest and cell death may be cell line specific. For instance, the BITC-induced cell cycle arrest and apoptosis induction in leukemia cells correlates with phosphorylation of Bcl-2 and activation of p38 mitogen-activated protein kinase and c-Jun NH_2-terminal kinase but not extracellular signal-regulated kinase 1/2 (14). On the other hand, the cell death caused by BITC in 1483 human head and neck cancer cell line is

Received 7/10/06; revised 8/18/06; accepted 9/12/06.

Grant support: USPHS grants CA101753 and CA115498, awarded by the National Cancer Institute.

The costs of publication of this article were defrayed in part by the payment of page charges. This article must therefore be hereby marked advertisement in accordance with 18 U.S.C. Section 1734 solely to indicate this fact.

Requests for reprints: Shivendra V. Singh, 2.32A Hillman Cancer Center Research Pavilion, 5117 Centre Avenue, Pittsburgh, PA 15213. Phone: 412-623-3263; Fax: 412-623-7828. E-mail: singhs@upmc.edu

doi:10.1158/1535-7163.MCT-06-0396

regulated by extracellular signal-regulated kinase 1/2 and p38 mitogen-activated protein kinase (12). Similarly, the BITC-mediated phosphorylation of Bcl-2 has been observed in some but not all cellular systems (11–17).

More recent epidemiologic studies have concluded that dietary intake of ITC-containing cruciferous vegetables may be protective against breast cancer (18, 19). For example, a case control study involving 337 breast cancer cases and matched controls (matched by age and menopausal status, date of urine collection, and day of laboratory assay) documented an inverse correlation between urinary levels of ITCs as a biological measure of cruciferous vegetable intake and breast cancer (odds ratio, 0.5 for 4th quartile; ref. 18). Similarly, Ambrosone et al. (19) have reported that consumption of cruciferous vegetables is marginally inversely associated with breast cancer risk in premenopausal women with 4th quartile odds ratio of 0.6 (95% confidence interval, 0.40-1.01; $P = 0.058$). This association was weaker or null among postmenopausal women (19). Despite compelling epidemiologic data, however, the efficacy of BITC or other ITC compounds against human breast cancer cells has not been systematically examined. Here, we show that BITC effectively suppresses growth of both estrogen-responsive (MCF-7) and estrogen-independent (MDA-MB-231) human breast cancer cell lines by causing G_2-M phase cell cycle arrest and apoptosis induction. Furthermore, we provide experimental evidence to indicate that the BITC-induced cell death in breast cancer cells is initiated by reactive oxygen species (ROS) and regulated by multidomain proapoptotic proteins Bax and Bak.

Materials and Methods

Reagents

BITC and phenethyl ITC (PEITC) were purchased from Aldrich (St. Louis, MO), whereas D,L-sulforaphane (SFN) was procured from LKT Laboratories (St. Paul, MN). Reagents for cell culture, including medium, penicillin and streptomycin antibiotic mixture, and serum, were purchased from Life Technologies (Grand Island, NY); propidium iodide, RNaseA, and 4′,6-diamidino-2-phenylindole (DAPI) were from Sigma-Aldrich; and hydroethidine and 6-carboxy-2′,7′-dichlorodihydrofluorescein diacetate (H_2DCFDA) were from Molecular Probes (Eugene, OR). The combined superoxide dismutase/catalase mimetic EUK134 was a generous gift from Eukarion (Bedford, MA). The antibodies against Bak, Bax, Bcl-xL, cyclin-dependent kinase (Cdk) 1, cell division cycle 25C (Cdc25C), and Smac/DIABLO were from Santa Cruz Biotechnology (Santa Cruz, CA), and the antibodies against cytochrome *c*, caspase-8, and caspase-9 were from PharMingen (Palo Alto, CA). The anti-Bcl-2 antibody was from DakoCytomation (Carpinteria, CA), the antibody against caspase-3 was from Cell Signaling Technology (Beverly, MA), and antibodies against cyclin B1 and actin were from Oncogene Research Products (San Diego, CA). The caspase inhibitors were from Enzyme Systems (Dublin, CA).

Cell Culture and Cell Survival Assay

The human breast cancer cell lines MDA-MB-231 and MCF-7 and the normal mammary epithelial cell line MCF-10A were procured from the American Type Culture Collection (Manassas, VA). Monolayer cultures of MDA-MB-231 cells were maintained in RPMI 1640 supplemented with 10% fetal bovine serum and antibiotics. Monolayer cultures of MCF-7 cells were maintained in MEM supplemented with 0.1 mmol/L nonessential amino acids, 1 mmol/L sodium pyruvate, 1.5 g/L sodium bicarbonate, 10% fetal bovine serum, and antibiotics. The nontumorigenic human mammary epithelial cell line MCF-10A was cultured in serum-free Mammary Epithelial Growth Medium (Clonetics, San Diego, CA) supplemented with 100 ng/mL cholera toxin (Calbiochem, La Jolla, CA). Mouse embryonic fibroblasts (MEF) derived from wild-type (WT), Bak knockout (Bak-KO), and Bax and Bak double knockout (DKO) mice and immortalized by transfection with a plasmid containing SV40 genomic DNA were generously provided by Dr. Stanley J. Korsmeyer (Dana-Farber Cancer Institute, Boston, MA) and maintained in DMEM supplemented with 10% heat-inactivated fetal bovine serum, 0.1 mmol/L nonessential amino acids, 0.1 μmol/L 2-mercaptoethanol, and antibiotics (20). Each cell line was maintained at 37°C in an atmosphere of 95% air and 5% CO_2. Stock solutions of the ITCs were prepared in DMSO, and an equal volume of DMSO (final concentration, 0.01–0.02%) was added to the controls. The effect of ITCs on cell survival was determined by trypan blue dye exclusion assay or sulforhodamine B assay following a 24-hour drug exposure as described by us previously (21, 22).

Analysis of Cell Cycle Distribution

The effect of BITC on cell cycle distribution was determined by flow cytometry after staining the cells with propidium iodide as described by us previously (23). Briefly, 5×10^5 cells were seeded in T25 flasks, allowed to attach by overnight incubation, and exposed to DMSO or desired concentration of BITC for specified times. Both floating and adherent cells were collected, washed with PBS, and fixed with 70% ethanol. The cells were then treated with RNaseA and propidium iodide for 30 minutes as described previously (23). The stained cells were analyzed using a Coulter Epics XL Flow Cytometer (Beckman Coulter, Miami, FL).

Immunoblotting

The cells were treated with BITC as described above, and both floating and attached cells were collected and lysed as described by us previously (23). The lysate proteins were resolved by 6% to 12.5% SDS-PAGE and transferred onto polyvinylidene fluoride membrane. The membrane was incubated with a solution containing TBS, 0.05% Tween 20, and 5% (w/v) nonfat dry milk. The membrane was treated with the desired primary antibody for 1 hour at room temperature or overnight at 4°C. Following treatment with appropriate secondary antibody, the immunoreactive bands were visualized using enhanced chemiluminescence method. The blots were

stripped and reprobed with anti-actin antibody to correct for differences in protein loading. The change in protein level was determined by densitometric scanning of the immunoreactive bands followed by correction for actin loading control.

Apoptosis Assays

The BITC-induced apoptosis was determined by (*a*) fluorescence microscopy following staining with DAPI, (*b*) quantitation of cytoplasmic histone-associated DNA fragmentation, or (*c*) flow cytometric analysis of cells with sub-G_0-G_1 DNA content following staining with propidium iodide. For DAPI assay, cells (2×10^4) were plated on coverslips, allowed to attach overnight, and exposed to DMSO or desired concentrations of BITC for specified times. The cells were washed with PBS and fixed with 3% paraformaldehyde for 1 hour at room temperature. The cells were washed thrice with PBS, permeabilized with 1% Triton X-100 for 4 minutes, washed again with PBS, and stained by incubation with 1 μg/mL DAPI for 5 minutes. The cells with condensed and fragmented DNA (apoptotic cells) were scored under a Leica DC300F fluorescence microscope (Wetzlar, Germany) at ×40 objective lens magnification. Cytoplasmic histone-associated DNA fragmentation was determined using a kit from Roche Applied Science (Mannheim, Germany) according to the manufacturer's recommendations. The sub-G_0-G_1 fraction was quantified as described previously (21, 23).

Measurement of Mitochondrial Membrane Potential

Mitochondrial membrane potential was measured using a potential-sensitive dye JC-1 (5,5′,6,6′-tetrachloro-1,1′,3,3′-tetraethyl-benzimidazolylcarbocyanine iodide). Stock solution of JC-1 (1 mg/mL) was prepared in DMSO and freshly diluted with the assay buffer. Briefly, cells (4×10^5) were plated in T25 flasks, allowed to attach overnight, exposed to desired concentrations of BITC for specified times, and collected by trypsinization. The cells were incubated with medium containing JC-1 (10 μg/mL) for 15 minutes at 37°C. The cells were washed with PBS, resuspended in 0.5 mL assay buffer, and analyzed using a Coulter Epics XL Flow Cytometer. Carbonyl cyanide 4-(trifluoromethoxy)-phenylhydrazone (FCCP; 25 μmol/L), an uncoupler of mitochondrial oxidative phosphorylation, was used as a positive control.

Transmission Electron Microscopy

Transmission electron microscopy was done essentially as described by us previously (24). Briefly, MDA-MB-231 cells (2×10^5) were plated in six-well plates and allowed to attach overnight. The cells were treated with DMSO (control) or 2.5 μmol/L BITC for 6 hours at 37°C. The cells were fixed in ice-cold 2.5% electron microscopy grade glutaraldehyde, rinsed with PBS, postfixed in 1% osmium tetroxide with 0.1% potassium ferricyanide, dehydrated through a graded series of ethanol (30–90%), and embedded in Epon (dodecenyl succinic anhydride, nadic methyl anhydride, scipoxy 812 resin, and dimethylaminomethyl; Energy Beam Sciences, East Granby, CT). Semithin (300 nm) sections were cut using a Reichart Ultracut, stained with 0.5% toluidine blue, and examined under a light microscope. Ultrathin sections (65 nm) were stained with 2% uranyl acetate and Reynold's lead citrate and examined on a JEOL 1210 transmission electron microscope (Peabody, MA) at ×10,000 and ×50,000 magnification.

Measurement of ROS

Intracellular ROS generation was measured by flow cytometry following staining with hydroethidine and H_2DCFDA as described by us previously (24). Briefly, cells (3×10^5) were plated in 60-mm culture dishes, allowed to attach overnight, and exposed to DMSO (control) or desired concentrations of BITC for specified time intervals. The cells were stained with 2 μmol/L hydroethidine and 5 μmol/L H_2DCFDA for 30 minutes at 37°C. The cells were collected and the fluorescence was measured using a Coulter Epics XL Flow Cytometer. In some experiments, cells were pretreated with 30 μmol/L EUK134 before BITC exposure and analysis of ROS generation.

Results

BITC Inhibited Survival of Cultured Human Breast Cancer Cells

We determined the effects of three widely studied ITC analogues (BITC, PEITC, and SFN) on cell survival using a pair of well-characterized human breast cancer cell lines (MDA-MB-231 and MCF-7) as a model. The MDA-MB-231 cell line, which was originally derived from a stage IV invasive ductal carcinoma, is estrogen receptor negative, partially proficient for all cell cycle checkpoints, and expresses mutant p53 (reviewed in ref. 25). The MCF-7 cell line, which is estrogen receptor positive and estrogen responsive, was isolated from a pleural effusion of stage IV invasive ductal carcinoma. The MCF-7 cells are aneuploid with high chromosomal instability and partially defective for the G_1 and mitotic spindle checkpoint but express normal p53 (25). The effect of ITC analogues on survival of MDA-MB-231 and MCF-7 cells was determined by trypan blue dye exclusion assay, and the results are summarized in Fig. 1A and B. The survival of MDA-MB-231 cells was decreased significantly on a 24-hour exposure to BITC in a concentration-dependent manner with a IC_{50} of <2.5 μmol/L. Moreover, BITC was relatively more effective than either PEITC or SFN against proliferation of MDA-MB-231 cells. For example, a 24-hour treatment of MDA-MB-231 cells with 5 μmol/L BITC resulted in an ~97% decrease in cell viability. On the other hand, about 24% and 56% of the MDA-MB-231 cells survived under similar conditions of PEITC and SFN treatment, respectively (Fig. 1A). The survival of MCF-7 cells was also decreased significantly in the presence of each ITC compound. However, the MCF-7 cell line was relatively less sensitive to growth inhibition by ITCs compared with MDA-MB-231. For instance, the survival of MCF-7 cells was decreased by about 37% and 54% on a 24-hour exposure to 2.5 and 5 μmol/L BITC, respectively (Fig. 1B). On the other hand, a similar BITC treatment

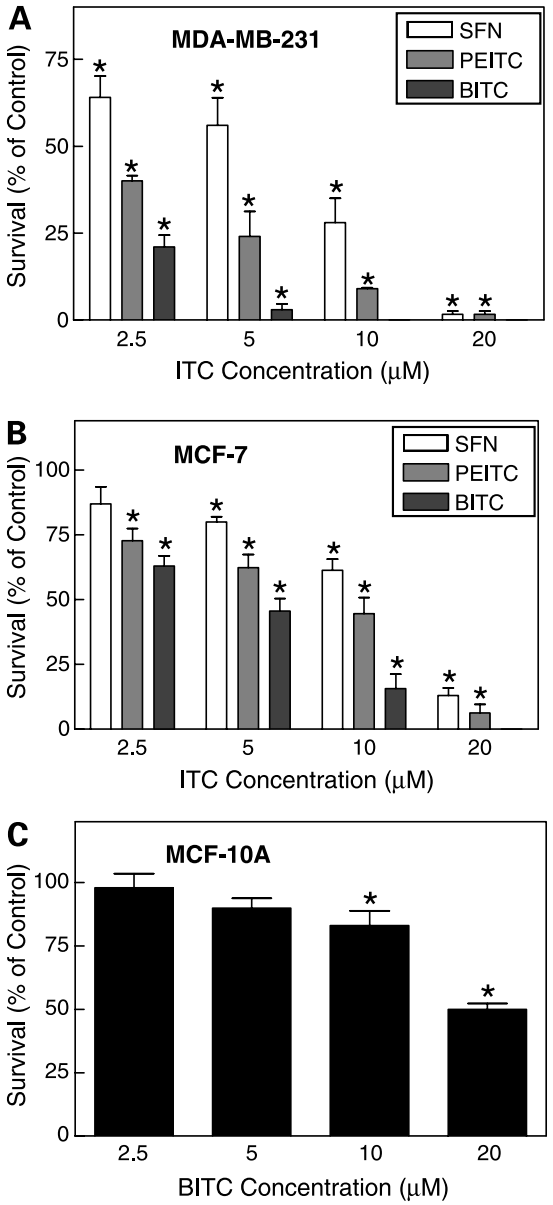

Figure 1. Effect of BITC, PEITC, and/or SFN treatment on survival of MDA-MB-231 (**A**), MCF-7 (**B**), and MCF-10A (**C**) cells as determined by trypan blue dye exclusion assay. The desired cell line was treated with DMSO (control) or indicated concentrations of the specified ITC compound for 24 h. *Columns,* mean ($n = 3$); *bars,* SE. *, $P < 0.05$, significantly different compared with DMSO-treated control by one-way ANOVA followed by Dunnett's test. Cell survival assay was performed twice in each cell line, and the results were comparable.

resulted in an approximately 79% to 97% inhibition of MDA-MB-231 cell viability (Fig. 1A). We selected BITC for further studies because of its higher potency compared with PEITC or SFN.

Next, we raised the question of whether BITC-mediated growth inhibition was selective toward cancer cells, which is a highly desirable feature of potential cancer preventive and therapeutic agents. We addressed this question by determining the effect of BITC treatment on viability of MCF-10A cells. The MCF-10A cell line is nontumorigenic in athymic mice and has been used extensively as a representative normal mammary epithelial cell line. The MCF-10A cell line was originally isolated from fibrocystic breast disease and was spontaneously immortalized (25). The MCF-10A cells have intact cell cycle checkpoints and normal proliferation controls (25). As can be seen in Fig. 1C, the MCF-10A cell line was significantly more resistant to growth inhibition by BITC compared with MDA-MB-231 or MCF-7 cells. For example, survival of MDA-MB-231 cells was decreased by ~97% on a 24-hour exposure to 5 μmol/L BITC (Fig. 1A). Viability of MCF-10A cells was inhibited by only ~10% by a similar BITC treatment (Fig. 1C). Collectively, these results indicated that the human breast cancer cells were significantly more sensitive to growth suppression by BITC compared with a normal mammary epithelial cell line.

BITC Treatment Caused G_2-M Phase Cell Cycle Arrest in Breast Cancer Cells

Cancer cell growth inhibition by many dietary agents, including ITCs and garlic-derived organosulfides, correlates with their ability to block cell cycle progression (23, 26, 27). To gain insights into the mechanism of growth-suppressive effect of BITC, we determined its effect on cell cycle distribution by flow cytometry following staining with propidium iodide. Representative histograms for cell cycle distribution in MDA-MB-231 cultures following a 24-hour exposure to DMSO (control) or 2.5 μmol/L BITC are shown in Fig. 2A. Exposure of MDA-MB-231 cultures to 1 and 2.5 μmol/L BITC for 24 hours resulted in statistically significant enrichment of sub-G_0-G_1 fraction, an indicator of DNA fragmentation, which was accompanied by a decrease in mainly G_0-G_1 and S phase cells (Fig. 2B). In addition, a 24-hour treatment of MDA-MB-231 cells with 2.5 μmol/L BITC caused an ~1.6-fold increase in G_2-M fraction compared with DMSO-treated control. The G_2-M phase cell cycle arrest was not evident at 0.5 or 1 μmol/L BITC concentration (Fig. 2B). In time course experiment using 2.5 μmol/L BITC, statistically significant enrichment of both sub-G_0-G_1 (Fig. 3A) and G_2-M fractions (Fig. 3B) was evident as early as 3 hours after treatment. The BITC-mediated enrichment of sub-G_0-G_1 fraction, but not the G_2-M population, increased progressively with increasing exposure time (Fig. 3A and B). These results indicated that the BITC-mediated inhibition of MDA-MB-231 cell survival was associated with a mild yet sustained G_2-M phase cell cycle arrest as well as DNA fragmentation (apoptosis).

To test whether the correlation between BITC-mediated cell growth inhibition and G_2-M phase cell cycle arrest observed in MDA-MB-231 was restricted to this cell line due to its unique genetic background, we determined the effect of BITC treatment on MCF-7 cell cycle distribution, and the results are summarized in Table 1. Similar to MDA-MB-231, BITC treatment (24 hours) caused a statistically significant increase in sub-G_0-G_1 as well as G_2-M fraction in MCF-7 cells. However, the BITC-mediated G_2-M phase cell cycle arrest was relatively more pronounced in MCF-7

cells (Table 1) than in MDA-MB-231 (Fig. 2B). For instance, compared with DMSO-treated control, the percentage of G_2-M fraction was increased by ~1.6-fold in MDA-MB-231 cells following a 24-hour treatment with 2.5 μmol/L BITC (Fig. 2B). A similar BITC treatment caused an ~2.6-fold increase in percentage of G_2-M fraction over control in MCF-7 cells (Table 1). The BITC-mediated G_2-M phase cell cycle arrest in MCF-7 cells was accompanied by a statistically significant decrease in G_0-G_1 and S phase cells at both 2.5 and 5 μmol/L concentrations ($P < 0.05$ by one-way ANOVA followed by Dunnett's test). Collectively, these results indicated that the BITC-mediated accumulation of subdiploid cells and G_2-M phase cell cycle arrest was not restricted to MDA-MB-231 cells.

To gain insights into the mechanism of BITC-mediated cell cycle arrest, we determined its effect on levels of proteins involved in regulation of G_2-M transition, including cyclin B1, Cdk1, and Cdc25C (28, 29), by immunoblotting, and the results are shown in Fig. 3C (MDA-MB-231) and Fig. 3D (MCF-7). The BITC treatment caused a decrease in protein levels of cyclin B1, Cdk1, and Cdc25C in both cell lines. The BITC-mediated decrease in protein levels of Cdk1 and Cdc25C was rapid and observed as early as 1 to 6 hours after treatment in both cell lines and coincided with the onset of G_2-M phase cell cycle arrest at least in MDA-MB-231 cells (Fig. 3B). These results indicated that the cell cycle arrest caused by BITC in MDA-MB-231 and MCF-7 cells was attributable to a decrease in protein levels of cyclin B1, Cdk1, and Cdc25C.

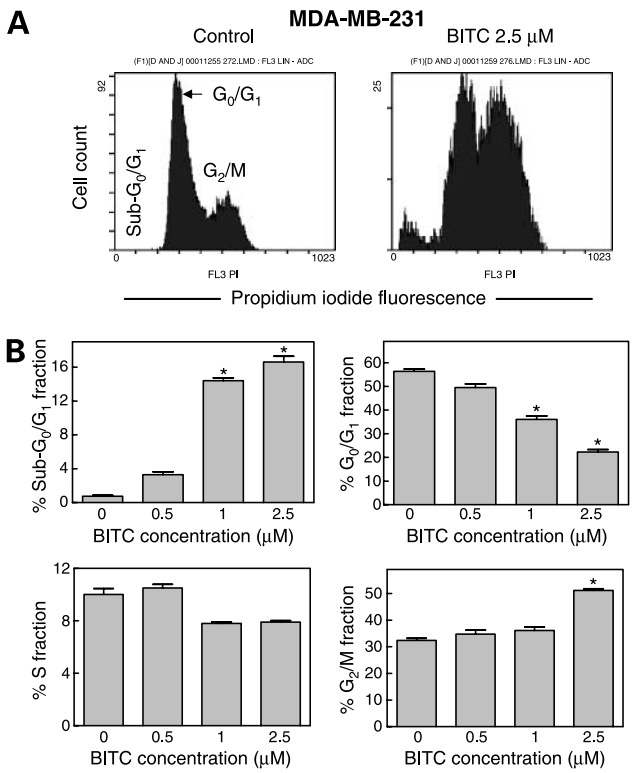

Figure 2. **A,** representative histograms depicting cell cycle distribution in MDA-MB-231 cultures following a 24-h treatment with DMSO (control) or 2.5 μmol/L BITC. **B,** cell cycle distribution in MDA-MB-231 cultures following a 24-h treatment with DMSO (control) or 0.5, 1, or 2.5 μmol/L BITC. *Columns,* mean ($n = 3$); *bars,* SE. *, $P < 0.05$, significantly different compared with DMSO-treated control by one-way ANOVA followed by Dunnett's test. Similar results were observed in two independent experiments.

Next, we determined the effect of BITC treatment on MCF-10A cell cycle distribution, and the results are summarized in Fig. 4. Representative histograms for cell cycle distribution in MCF-10A cultures treated for 24 hours with DMSO (control) or 20 μmol/L BITC are shown in Fig. 4A. In contrast to MDA-MB-231 and MCF-7 cells, BITC treatment failed to cause G_2-M phase cell cycle arrest in MCF-10A cells (Fig. 4B). Collectively, these results indicated that the breast cancer cells were more sensitive to BITC-mediated inhibition of cell cycle progression compared with the MCF-10A normal mammary epithelial cell line.

BITC Treatment Caused Apoptosis in Breast Cancer Cells

Analysis of cell cycle distribution suggested that BITC treatment might cause apoptosis in both MDA-MB-231 and MCF-7 cells as revealed by accumulation of subdiploid cells (Fig. 2B; Table 1), which is a characteristic feature of cells undergoing apoptosis. Apoptosis (also known as programmed cell death) is a tightly regulated process of cellular suicide that is characterized by several morphologic and cellular changes, including chromatin condensation, membrane blebbing, DNA fragmentation, and cleavage of key cellular proteins (30). Apoptosis induction by BITC was assessed by fluorescence microscopy after staining with DAPI. Representative DAPI staining in cultures of MDA-MB-231 cells following a 24-hour treatment with DMSO (control) or 2.5 μmol/L BITC is depicted in Fig. 5A. The BITC treatment caused a statistically significant increase in apoptotic cells, which were rarely seen in DMSO-treated MDA-MB-231 cultures (Fig. 5A). Apoptotic cells with condensed and fragmented DNA were scored from control (DMSO, 24 hours) and BITC-treated (1 and 2.5 μmol/L BITC, 24 hours) MDA-MB-231 cultures, and the results are summarized in Fig. 5B. The percentage of apoptotic cells was increased by about 8.5- and 11.3-fold on a 24-hour treatment with 1 and 2.5 μmol/L BITC, respectively, compared with DMSO-treated control (Fig. 5B). Apoptosis induction by BITC in MDA-MB-231 cells was confirmed by analysis of cytoplasmic histone-associated DNA fragmentation, which has emerged as yet another sensitive technique for quantitation of apoptotic cell death. A 24-hour exposure of MDA-MB-231 cells to BITC resulted in a concentration-dependent and statistically significant increase in cytoplasmic histone-associated DNA fragmentation when compared with control. For instance, the cytoplasmic histone-associated DNA fragmentation was increased by about 1.9- and 3.1-fold on a 24-hour treatment of MDA-MB-231 cells with 1 and 5 μmol/L BITC, respectively, relative to DMSO-treated control (Fig. 5C). The BITC-mediated cytoplasmic histone-associated DNA fragmentation was also evident in MCF-7

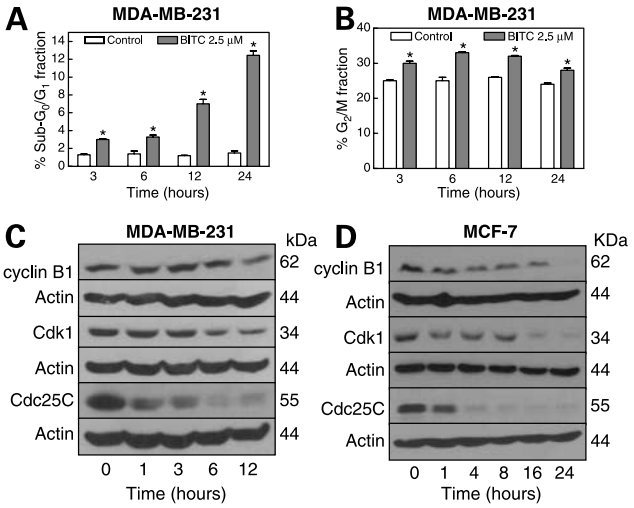

Figure 3. A time course study for effect of 2.5 μmol/L BITC on percentage of sub-G_0-G_1 population (**A**) and G_2-M fraction (**B**) in MDA-MB-231 cells. Control cells were exposed to DMSO. *Columns*, mean (n = 3); *bars*, SE. *, $P < 0.05$, significantly different compared with corresponding DMSO-treated control by paired t test. **C,** immunoblotting for cyclin B1, Cdk1, and Cdc25C using lysates from MDA-MB-231 cells cultured in the presence of 2.5 μmol/L BITC for the indicated times. **D,** immunoblotting for cyclin B1, Cdk1, and Cdc25C using lysates from MCF-7 cells cultured in the presence of 10 μmol/L BITC for the indicated times. The blots were stripped and reprobed with anti-actin antibody as a loading control.

cells, although a relatively higher concentration of BITC (>2 μmol/L) was required to observe statistically significant effect (Fig. 5D). In agreement with cell survival data, the MCF-10A cell line was resistant to apoptosis induction by BITC compared with the breast cancer cells (Fig. 5E). For instance, even at 20 μmol/L concentration, the BITC-mediated cytoplasmic histone-associated DNA fragmentation was increased only by ~55% in MCF-10A cells (Fig. 5E). Collectively, these results indicated that BITC treatment caused apoptosis in both MDA-MB-231 and MCF-7 cells.

Effect of BITC Treatment on Levels of Bcl-2 Family Proteins

The Bcl-2 family proteins have emerged as critical regulators of apoptosis by functioning as either promoters (e.g., Bax and Bak) or inhibitors (e.g., Bcl-2 and Bcl-xL) of the cell death process (20, 31, 32). We determined the effect of BITC treatment on levels of Bcl-2 family proteins by immunoblotting to gain insights into the mechanism of BITC-induced apoptosis in our model, and representative blots are shown in Fig. 6A (MDA-MB-231) and Fig. 6B (MCF-7). The level of multidomain proapoptotic protein Bax was increased by BITC treatment only in MCF-7 cells. On the other hand, BITC treatment resulted in an increase in the level of Bak protein in both MDA-MB-231 and MCF-7 cells. For instance, the protein level of Bak was increased by ~10-fold following an 8-hour treatment of MDA-MB-231 cells with 2.5 μmol/L BITC (Fig. 6A) as revealed by densitometric scanning of the immunoreactive bands and corrected for actin loading control. The BITC treatment also caused a decrease in protein levels of Bcl-2 and Bcl-xL in MDA-MB-231 cells. Interestingly, BITC treatment resulted in an increase in Bcl-xL protein level in MCF-7 cells especially at 16- to 24-hour time points. Collectively, these results indicated that BITC treatment differentially altered the levels of Bcl-2 family proteins in MDA-MB-231 and MCF-7 cells.

Bak and Bax Deficiency Conferred Protection against BITC-Induced Apoptosis

Because BITC treatment caused an increase in the level of Bak protein in both MDA-MB-231 and MCF-7 cells (Fig. 6A and B), we hypothesized that Bak might play an important role in regulation of BITC-induced apoptosis. We tested this hypothesis by comparing sensitivities of SV40-immortalized MEFs derived from WT, Bak-KO, and DKO mice toward BITC-induced apoptosis. The BITC treatment caused a concentration-dependent and statistically significant increase in apoptotic cell death in WT MEFs as judged by analysis of subdiploid fraction (Fig. 6C) and cytoplasmic histone-associated DNA fragmentation (Fig. 6D). On the other hand, the MEFs derived from Bak-KO and DKO mice were significantly more resistant to BITC-induced apoptosis compared with WT MEFs. For instance, a 16-hour treatment of WT MEFs with 2.5 μmol/L BITC resulted in ~32-fold increase in percentage of subdiploid cells when compared with DMSO-treated control (Fig. 6C). The percentage of subdiploid cells was increased by only about 5- to 9-fold by a similar BITC treatment in MEFs derived from Bak-KO and DKO mice (Fig. 6C). Taken together, these results clearly indicated that Bak protein might play an important role in regulation of BITC-induced apoptosis.

BITC Treatment Caused Cytosolic Release of Apoptogenic Molecules

Bak and Bax proteins are thought to contribute to the cell death process by promoting release of apoptogenic molecules from mitochondria to the cytosol. Because Bak and Bax deficiency conferred significant protection against BITC-induced apoptosis (Fig. 6C and D), we sought to determine whether the cell death caused by BITC was associated with disruption of the mitochondrial membrane potential. The effect of BITC treatment on mitochondrial membrane potential was determined by

Table 1. Effect of BITC treatment on MCF-7 cell cycle distribution

BITC concentration	Percent cells in phase			
	Sub-G_0-G_1	G_0-G_1	S	G_2-M
Control (DMSO)	3 ± 0.6	58 ± 0.6	19 ± 0.2	21 ± 1.0
2.5 μmol/L	16 ± 0.2*	20 ± 1.3*	9 ± 0.6*	55 ± 1.9*
5 μmol/L	12 ± 0.6*	19 ± 0.7*	8 ± 0.1*	61 ± 0.8*

NOTE: Results are mean ± SE (n = 3).
*$P < 0.05$, significantly different compared with DMSO-treated control by one-way ANOVA followed by Dunnett's test. Similar results were observed in two independent experiments.

flow cytometry following staining with a potential sensitive dye JC-1. The JC-1 dye bearing a delocalized positive charge enters the mitochondrial matrix due to the negative charge established by the intact mitochondrial membrane potential (33). In healthy cells, JC-1 dye stains the mitochondria red due to formation of J-aggregates (33). In apoptotic cells, JC-1 dye accumulates in the cytoplasm in monomeric form (green fluorescence) due to collapse of the mitochondrial membrane potential (33). Representative histograms for red and green fluorescence in MDA-MB-231 cells following a 6-hour treatment with DMSO (control), 2.5 μmol/L BITC, or a positive control (FCCP) are shown in Fig. 7A. In DMSO-treated control MDA-MB-231 cells, mitochondria predominantly exhibited red fluorescence due to accumulation of J-aggregates, indicating intact mitochondrial membrane potential. The BITC treatment disrupted mitochondrial membrane potential as revealed by an increase in green fluorescence resulting from cytosolic accumulation of monomeric JC-1. In time course experiments using 2.5 μmol/L BITC, the disruption of MDA-MB-231 mitochondrial membrane potential was evident as early as 1 hour after treatment (Fig. 7B). The BITC-mediated disruption of the mitochondrial membrane potential was also evident in MCF-7 cells (Fig. 7C). To determine if BITC-mediated disruption of the mitochondrial membrane potential was accompanied by cytosolic release of apoptogenic molecules, mitochondria-free cytosolic fractions were prepared from control and BITC-treated (2.5 μmol/L) MDA-MB-231 cells for immunoblotting of cytochrome *c* and Smac/DIABLO. As can be seen in Fig. 7D, BITC treatment caused a marked increase in cytosolic levels of both cytochrome *c* and Smac/DIABLO that was evident as early as 1 hour after treatment. The BITC-mediated release of cytochrome *c* from mitochondria to the cytosol was also observed in MCF-7 cells (results not shown).

Next, we determined the effect of BITC treatment (2.5 μmol/L, 6 hours) on mitochondrial morphology by transmission electron microscopy using MDA-MB-231 cells, and representative micrographs are shown in Fig. 8. We selected 6 hours of treatment for electron microscopy because BITC-mediated disruption of the mitochondrial membrane potential and cytosolic release of apoptogenic molecules was clearly evident at this time point (Fig. 7). As can be seen in Fig. 8, the DMSO-treated control MDA-MB-231 cells exhibited a normal complement of healthy-looking mitochondria. Although the mitochondria of BITC-treated MDA-MB-231 cells otherwise appeared normal, the BITC treatment caused appearance of large membranous vacuoles in the cytoplasm (identified by arrows). Some of these membranous vacuoles resembled autophagosomes and contained remnants of degraded organelles, including mitochondria (identified by arrows). Moreover, the BITC-treated cells exhibited chromatin condensation and membrane blebbing (identified by an arrowhead), which are characteristic features of cells engaged in apoptosis. Collectively, these results indicated that BITC treatment disrupted mitochondrial membrane potential, leading to release of apoptogenic molecules from mitochondria to the cytosol without causing any visible changes in mitochondrial morphology, such as swelling. In addition, we found that BITC treatment caused formation of autophagosome-like structures at least in MDA-MB-231 cells.

BITC-Induced Apoptosis Was Dependent on ROS Generation

Previous studies have shown that BITC-induced cell death in a rat liver epithelial cell line RL34 is associated with generation of ROS. However, it is unclear if the BITC-induced cell death in cancer cells is also initiated by ROS production. We therefore designed experiments to investigate possible role of ROS in BITC-induced apoptosis in our model. Intracellular ROS generation in control (DMSO treated) and BITC-treated MDA-MB-231 cells was assessed by flow cytometry following staining with hydroethidine and H_2DCFDA, which are somewhat specific for detection of superoxide anion and peroxides (e.g., H_2O_2), respectively (34, 35). The hydroethidine is oxidized to ethidium bromide, whereas H_2DCFDA is cleaved by nonspecific cellular esterases and oxidized in the presence of H_2O_2 and other peroxides to yield fluorescent 2′,7′-dichlorofluorescein (DCF). Representative histograms for ethidium

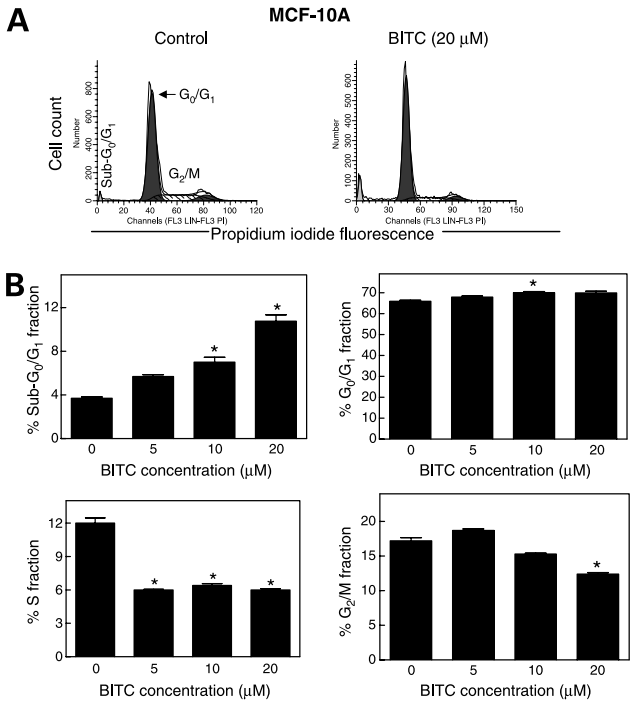

Figure 4. **A,** representative histograms depicting cell cycle distribution in MCF-10A cultures following a 24-h treatment with DMSO (control) or 20 μmol/L BITC. **B,** cell cycle distribution in MCF-10A cultures following a 24-h treatment with DMSO (control) or 5, 10, or 20 μmol/L BITC. *Columns,* mean (n = 3); *bars,* SE. *, $P < 0.05$, significantly different compared with DMSO-treated control by one-way ANOVA followed by Dunnett's test. Similar results were observed in two independent experiments.

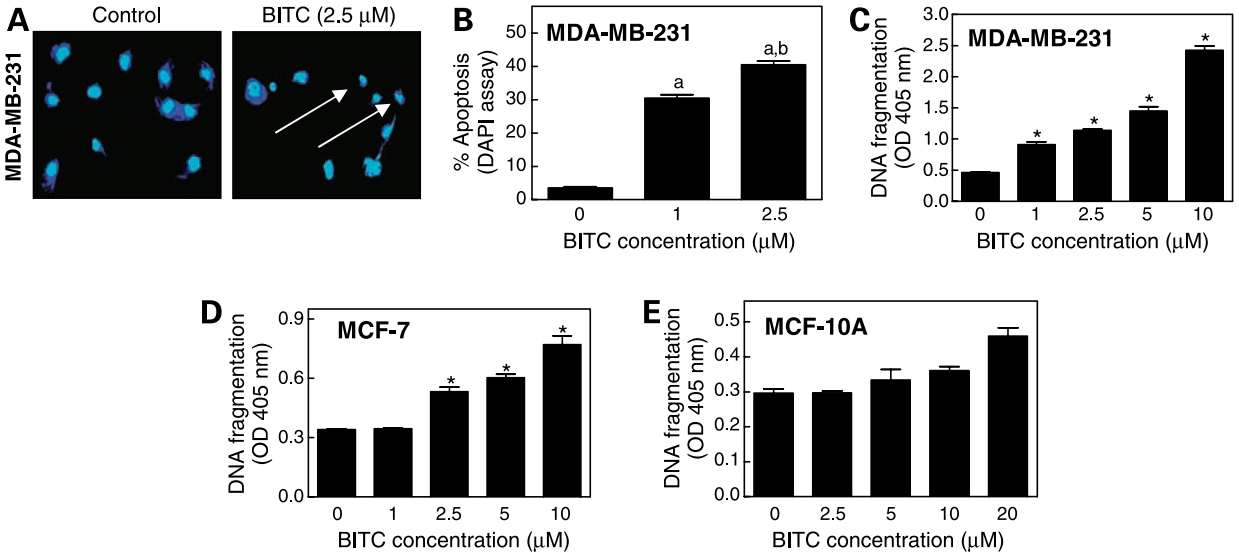

Figure 5. **A,** DAPI staining for MDA-MB-231 cultures treated for 24 h with DMSO or 2.5 μmol/L BITC. Apoptotic cells with condensed chromatin (*arrows*) were clearly visible in BITC-treated culture but much less frequent in DMSO-treated controls. **B,** quantitation of apoptotic cells with condensed chromatin (DAPI assay) in MDA-MB-231 cultures following a 24-h treatment with DMSO (control) or BITC (1 or 2.5 μmol/L). *Columns,* mean of six to nine determinations; *bars,* SE. [a], $P < 0.05$, significantly different compared with DMSO-treated control; [b], $P < 0.05$, significantly different compared with 1 μmol/L BITC by one-way ANOVA followed by Bonferroni's multiple comparison test. Cytoplasmic histone-associated DNA fragmentation in MDA-MB-231 (**C**), MCF-7 (**D**), and MCF-10A (**E**) cells following a 24-h treatment with DMSO (control) or the indicated concentrations of BITC. **C** to **E,** *columns,* mean ($n = 3$ for MDA-MB-231 and MCF-7 cells and $n = 2$ for MCF-10A cells; the error bars in MCF-10A are shown to indicate range of values). *, $P < 0.05$, significantly different compared with DMSO-treated control by one-way ANOVA followed by Dunnett's test. Similar results were observed in two independent experiments.

bromide and DCF fluorescence in MDA-MB-231 cells treated for 2 hours with either DMSO (control) or 2.5 μmol/L BITC are depicted in Fig. 9A. The BITC-treated MDA-MB-231 cells exhibited a time-dependent increase in DCF fluorescence compared with control (Fig. 9B). The BITC-mediated increase in DCF fluorescence was evident as early as 1 hour after treatment and peaked between 2 and 4 hours after drug treatment (Fig. 9B). For instance, the DCF fluorescence in MDA-MB-231 cells treated for 1 and 2 hours with 2.5 μmol/L BITC was increased by about 4.2- and 5.0-fold, respectively, compared with vehicle-treated control (Fig. 9B). Interestingly, a similar BITC treatment in nontumorigenic MCF-10A cell line failed to cause ROS generation (results not shown). However, the BITC-mediated ROS generation was observed in MCF-7 cells (results not shown).

Next, we raised the question of whether ROS production contributed to the cell death caused by BITC in breast cancer cells. We addressed this question by determining the effect of a combined superoxide dismutase and catalase mimetic (EUK134) on BITC-induced ROS generation, apoptosis induction, and cell survival. As can be seen in Fig. 10A, a 2-hour exposure of MDA-MB-231 cells to 2.5 μmol/L BITC resulted in an ~2.3-fold increase in DCF fluorescence compared with DMSO-treated control, which was reduced to below control level in the presence of EUK134. In addition, EUK134 conferred partial yet statistically significant protection against BITC-induced apoptosis as revealed by cytoplasmic histone-associated DNA fragmentation assay (Fig. 10B) and cell survival as revealed by sulforhodamine B assay (Fig. 10C). Similar to MDA-MB-231 cells, EUK134 conferred partial but statistically significant protection against BITC-induced ROS production (Fig. 10D) and cytoplasmic histone-associated DNA fragmentation (Fig. 10E) in MCF-7 cells as well. Collectively, these results indicated that BITC-induced apoptosis in breast cancer cells was partially dependent on ROS production.

Involvement of Caspases in BITC-Induced Apoptosis

Caspases are aspartate-specific cysteine proteases that play critical roles in execution of apoptosis program (36, 37). Activation of caspases results in cleavage and inactivation of key cellular proteins (36, 37). Next, we explored the possibility of whether BITC-induced cell death was mediated by caspases. As can be seen in Fig. 11, treatment of MDA-MB-231 cells with 2.5 μmol/L BITC resulted in cleavage of procaspase-3 that was evidenced by appearance of 17- and 19-kDa cleaved intermediates (Fig. 11A, *arrowheads*). In addition, BITC treatment caused a decrease in the levels of procaspase-9 and procaspase-8 that was accompanied by appearance of cleaved 37-kDa (caspase-9) and 43-kDa (caspase-8) intermediates (Fig. 11B, *arrowheads*). We used pharmacologic inhibitors of caspases to confirm their involvement in BITC-induced apoptosis. As shown in Fig. 12A, the BITC-mediated cleavage of procaspase-3 was attenuated in the presence of pan-caspase inhibitor zVAD-fmk as well as specific inhibitors of caspase-9 (zLEHD-fmk)

and caspase-8 (zIETD-fmk). Consistent with these results, the BITC-induced cytoplasmic histone-associated DNA fragmentation was also significantly attenuated in the presence of zVAD-fmk, zLEHD-fmk, and zIETD-fmk (Fig. 12B). These results pointed toward involvement of both caspase-8 and caspase-9 pathways in execution of BITC-induced apoptosis.

Discussion

The present study reveals that the cruciferous vegetable-derived ITCs, especially BITC, effectively suppress growth of MDA-MB-231 and MCF-7 cells, whereas a normal mammary epithelial cell line (MCF-10A) is somewhat resistant to growth inhibition by BITC. These results suggest that BITC may selectively target breast cancer cells but spare normal breast epithelium, which is a highly desirable property of potential anticancer agents. Growth inhibitory effect of BITC has been observed previously in other types of cancer cells, including head and neck squamous cell carcinoma and pancreatic cancer cells (12, 13). However, the breast cancer cells used in the present study seem relatively more sensitive to growth inhibition by BITC compared with other types of cancer cells. For instance, the IC_{50} of BITC for MDA-MB-231 (<2.5 μmol/L; Fig. 1A) is considerably lower than that for human head and neck squamous cell carcinoma 1483 and UM-22B (IC_{50}, ~17–22 μmol/L; ref. 12) and Jurkat leukemia (IC_{50}, ~6 μmol/L; ref. 14).

Cellular effects of BITC (e.g., cell killing, ROS generation, disruption of the mitochondrial membrane potential, and apoptosis) in MDA-MB-231 cells are evident at 1 to 2.5 μmol/L concentrations. Although pharmacokinetics for BITC has not been systematically investigated, the maximal plasma concentration of its close structural analogue PEITC (C_{max}) following ingestion of 100 g watercress ranges between 673 and 1,155 nmol/L (mean, 928 ± 250 nmol/L) with t_{max} (time to reach C_{max}) of ~2.1 ± 1.1 hours (38). A C_{max} between 0.64 and 1.4 μmol/L (mean, 1.04 ± 0.22 μmol/L) of total ITC in three subjects taking a single dose of PEITC (40 mg) was reported in another study (39). Thus, it is possible that the BITC concentrations required to produce statistically significant inhibition of human breast cancer cell growth may be achievable *in vivo*.

Similar to other cellular systems (11–17), the BITC-mediated growth inhibition of cultured breast cancer cells correlates with G_2-M phase cell cycle arrest and apoptosis induction. In our model, BITC treatment causes a

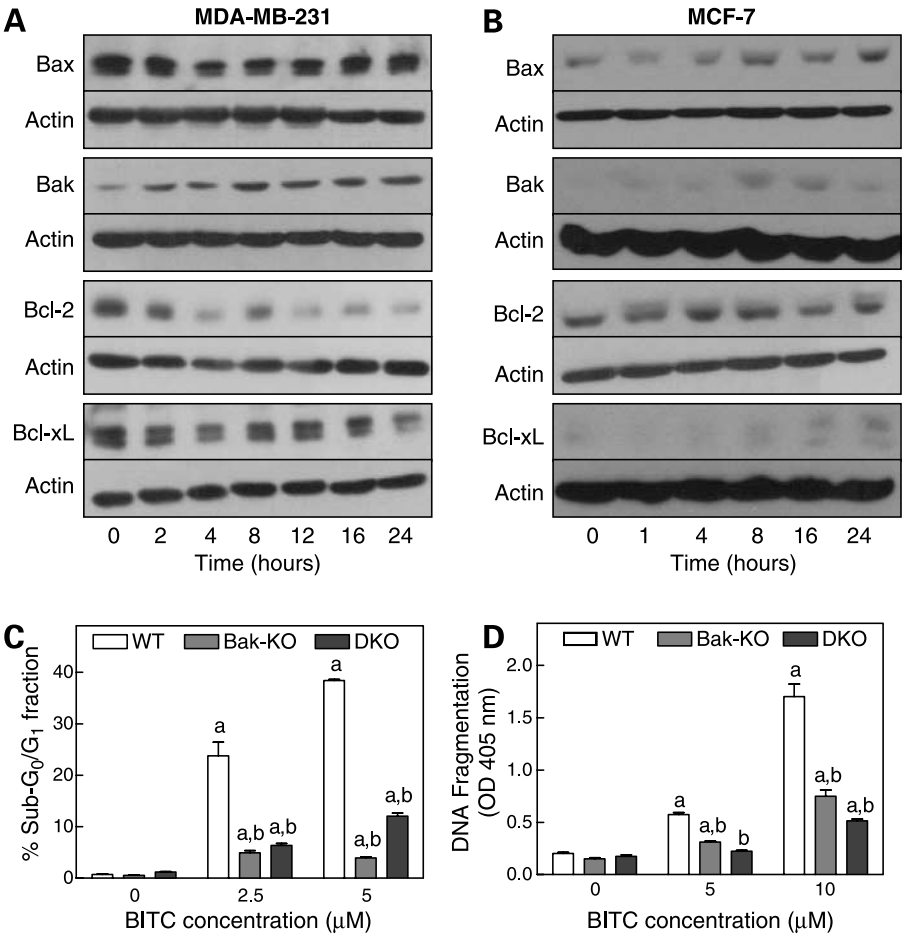

Figure 6. **A,** immunoblotting for Bcl-2 family proteins using lysates from MDA-MB-231 cells cultured in the presence of 2.5 μmol/L BITC for the indicated times. **B,** immunoblotting for Bcl-2 family proteins using lysates from MCF-7 cells cultured in the presence of 10 μmol/L BITC for the indicated times. The blots were stripped and reprobed with anti-actin antibody as a loading control. **C,** percentage of subdiploid fraction in cultures of WT, Bak-KO, and DKO following a 16-h treatment with DMSO (control) or the indicated concentrations of BITC. *Columns,* mean (n = 3); *bars,* SE. [a], $P < 0.05$, significantly different compared with corresponding DMSO-treated control; [b], $P < 0.05$, significantly different compared with WT MEFs by one-way ANOVA followed by Bonferroni's multiple comparison test. **D,** cytoplasmic histone-associated DNA fragmentation in WT, Bak-KO, and DKO MEFs following a 24-h treatment with DMSO (control) or the indicated concentrations of BITC. *Columns,* mean (n = 3); *bars,* SE. [a], $P < 0.05$, significantly different compared with corresponding DMSO-treated control; [b], $P < 0.05$, significantly different compared with WT MEFs by one-way ANOVA followed by Bonferroni's multiple comparison test. Similar results were observed in two independent experiments.

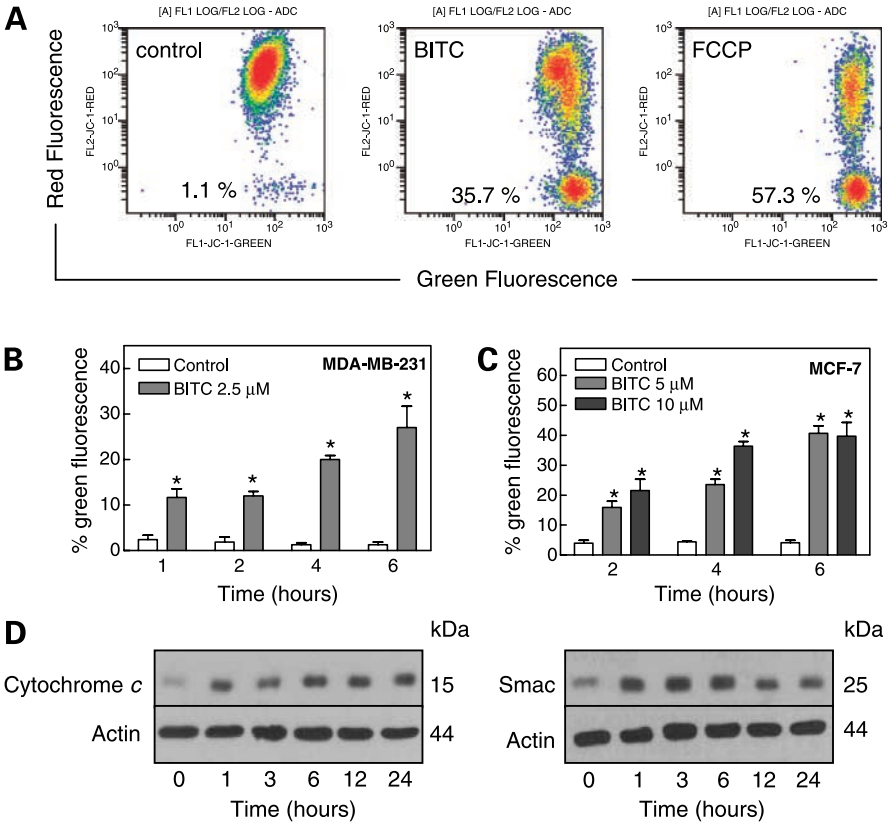

Figure 7. **A,** representative flow histograms depicting JC-1 fluorescence in MDA-MB-231 cells following a 6-h treatment with DMSO (control) or 2.5 μmol/L BITC or 25 μmol/L FCCP (positive control). Note an increase in green fluorescence in FCCP-treated (positive control) and BITC-treated MDA-MB-231 cells. **B,** percentage of cells with green fluorescence in MDA-MB-231 cultures treated with DMSO or 2.5 μmol/L BITC for the indicated times. *Columns,* mean ($n = 3$); *bars,* SE. *, $P < 0.05$, significantly different compared with corresponding DMSO-treated control by paired *t* test. Similar results were observed in two independent experiments. **C,** percentage of cells with green fluorescence in MCF-7 cultures treated with DMSO or BITC (5 or 10 μmol/L) for the indicated times. *Columns,* mean ($n = 3$); *bars,* SE. *, $P < 0.05$, significantly different compared with corresponding DMSO-treated control by one-way ANOVA followed by Dunnett's test. **D,** immunoblotting for cytochrome *c* and Smac/DIABLO using mitochondria-free cytosolic fractions prepared from MDA-MB-231 cells following treatment with 2.5 μmol/L BITC for the indicated times. Blots were stripped and reprobed with anti-actin antibody as a loading control.

concentration-dependent enrichment of subdiploid apoptotic cells and G_2-M fraction in both MDA-MB-231 and MCF-7 cell lines. On the other hand, the MCF-10A normal mammary epithelial cell line is significantly more resistant to cell cycle arrest and apoptosis induction by BITC compared with breast cancer cells, which may explain the relative insensitivity of MCF-10A cells to growth suppression by this ITC compound. Previous studies have suggested that BITC-induced cell cycle arrest and apoptosis induction may be interrelated events because the G_2-M phase-arrested Jurkat cells are more sensitive to undergoing apoptotic stimulation by BITC than the cells in other phases (14). Based on the results of our dose-response studies (Figs. 2B and 5C), we propose that the BITC-mediated cell cycle arrest and apoptosis in our model may be separate responses. For instance, the BITC-mediated apoptosis (enrichment of subdiploid fraction as well as cytoplasmic histone-associated DNA fragmentation) in MDA-MB-231 cells is evident at 1 μmol/L concentration, whereas a higher BITC concentration (2.5 μmol/L) is needed to observe G_2-M phase cell cycle arrest. The time course kinetic studies also support the notion that cell cycle arrest and apoptosis may be independent responses to BITC at least in MDA-MB-231 cells because a time-dependent increase is noticeable in subdiploid fraction but not G_2-M phase cells (Fig. 3A and B).

Previous studies have concluded that p53 tumor suppressor is necessary for apoptosis induction by PEITC because the MEFs derived from p53 knockout mice are resistant to the cell death caused by PEITC (40). The p53 tumor suppressor, which is transcriptionally inert in the absence of stress, is involved in regulation of apoptosis by different stimuli (41, 42). The p53 protein is stabilized under stress and transcriptionally regulates the expression of certain genes involved in apoptosis signaling, such as Bax (41, 42). The present study reveals that p53 is not required for BITC-induced apoptosis at least in our model because the cell death is observed both in MDA-MB-231, which expresses mutant p53, as well as in WT p53-expressing cell line MCF-7. On the other hand, the p53 status may be a contributing factor in differential response of MDA-MB-231 and MCF-7 cells to BITC-induced G_2-M phase cell cycle arrest. This conclusion is based on the following observations: (*a*) the BITC-mediated G_2-M phase cell cycle arrest is relatively more pronounced in MCF-7 cell line than in the MDA-MB-231 (compare Fig. 2B and Table 1), (*b*) both *cdk1* and *cyclin B1* genes are transcriptionally repressed by p53 (reviewed in ref. 43), and (*c*) the BITC-mediated down-modulation of both Cdk1 and cyclin B1 proteins is relatively more pronounced in MCF-7 cell line than in the MDA-MB-231 (Fig. 3C and D).

Eukaryotic cell cycle progression involves sequential activation of Cdks whose activation is dependent on their association with regulatory cyclins (28). A complex formed by the association of Cdk1 (also known as $p34^{cdc2}$) with

cyclin B1 plays a major role in regulation of G_2-M transition (28). Activity of Cdk1/cyclin B1 kinase complex is negatively regulated by reversible phosphorylations at Thr^{14} and Tyr^{15} of Cdk1 (28). Dephosphorylation of Thr^{14} and Tyr^{15} of Cdk1 and hence activation of Cdk1/cyclin B1 kinase complex is catalyzed by Cdc25 family of dual-specificity phosphatases, and this reaction is believed to be the rate-limiting step for entry into mitosis (29). The BITC-mediated inhibition of G_2-M progression in both MDA-MB-231 and MCF-7 cells is associated with a decrease in the protein levels of Cdk1, cyclin B1, and Cdc25C, albeit to a greater extent in MCF-7 than in the MDA-MB-231 cell line. Thus, it is reasonable to postulate that the BITC-mediated cell cycle arrest in our model is likely due to inhibition of complex formation between Cdk1 and cyclin B1 and/or sustained Thr^{14} and Tyr^{15} phosphorylation (inactivation) of Cdk1/cyclin B1 kinase complex due to down-regulation of Cdc25C protein. The BITC-mediated G_2-M phase cell cycle arrest in association with down-modulation of Cdk1, cyclin B1, and Cdc25B has also been reported in a pancreatic cancer cell line (13).

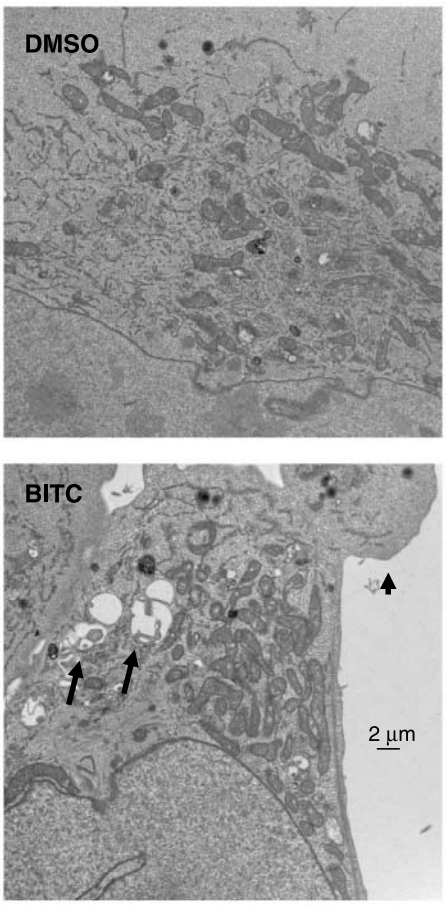

Figure 8. Representative transmission electron micrographs (×10,000 magnification) of MDA-MB-231 following a 6-h treatment with DMSO or 2.5 μmol/L BITC. Note the abundance of membranous vacuoles (*arrows*) in BITC-treated MDA-MB-231 cells, which were rarely seen in DMSO-treated controls. Some of these vacuoles resembled autophagosomes and contained remnants of mitochondria. The BITC-treated cells also exhibited chromatin condensation and membrane blebbing (*arrowhead*), which are characteristic features of cells undergoing apoptosis.

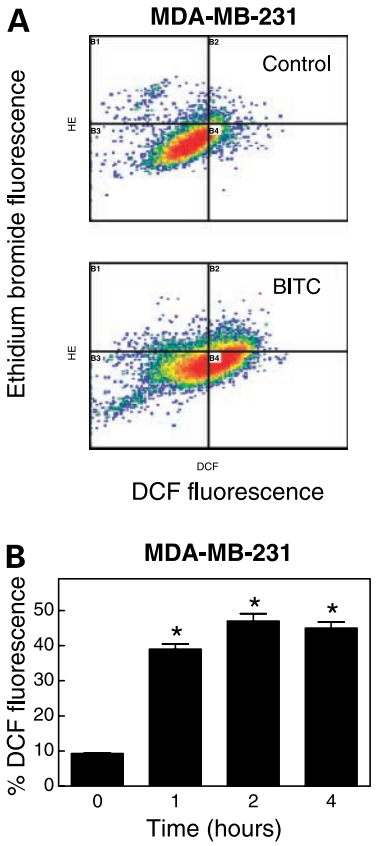

Figure 9. **A,** representative histograms depicting ethidium bromide fluorescence (an indicator of superoxide anion production) and DCF fluorescence (an indicator of peroxide production) in MDA-MB-231 cells following a 2-h treatment with DMSO (control) or 2.5 μmol/L BITC. **B,** percentage of cells with DCF fluorescence in MDA-MB-231 cultures treated with DMSO (control) or 2.5 μmol/L BITC for the indicated times. *Columns,* mean (n = 3); *bars,* SE. *, $P < 0.05$, significantly different compared with DMSO-treated control by one-way ANOVA followed by Dunnett's test. The experiment was repeated twice, and representative data from a single experiment are shown.

The Bcl-2 family proteins have emerged as critical regulators of the mitochondria-mediated apoptosis by functioning as either promoters (e.g., Bax and Bak) or inhibitors (e.g., Bcl-2 and Bcl-xL) of the cell death process (31, 32, 44, 45). Antiapoptotic Bcl-2 family members (Bcl-2 and Bcl-xL) possess four conserved BH domains (BH1, BH2, BH3, and BH4) and mainly prevent the release of apoptogenic molecules (e.g., cytochrome *c*) from mitochondria to the cytosol by forming heterodimer complexes with proapoptotic family members, such as Bax (31, 32, 44, 45). The proapoptotic Bcl-2 family proteins, which can be subdivided into the Bax subfamily of multidomain proteins (e.g., Bax and Bak) or BH3-only subfamily (e.g., Bid and Bim), induce mitochondrial membrane

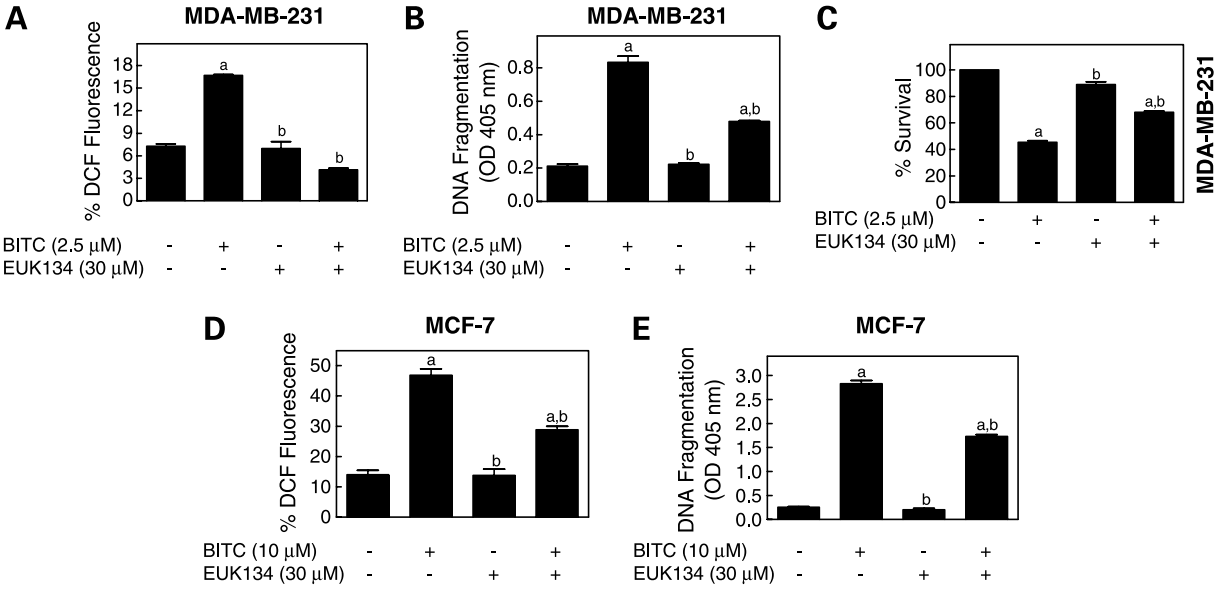

Figure 10. Effect of combined superoxide dismutase and catalase mimetic EUK134 on BITC-induced ROS generation (**A** and **D**), cytoplasmic histone-associated DNA fragmentation (**B** and **E**), and cell killing (**C**) in MDA-MB-231 cells (**A**–**C**) and MCF-7 cells (**D**–**E**). Desired cell line was allowed to attach overnight and exposed to either DMSO or 30 μmol/L EUK134 for 1 to 2 h. The cells were then either left untreated (DMSO and EUK134 alone treatment group) or exposed to BITC (2.5 μmol/L for MDA-MB-231 and 10 μmol/L for MCF-7) for desired time point (2 or 4 h for ROS production assay and 16 or 24 h for cytoplasmic histone-associated DNA fragmentation and cell survival assays). *Columns,* mean (n = 3); *bars,* SE. [a], $P < 0.05$, significantly different compared with control; [b], $P < 0.05$, significantly different compared with BITC alone treatment group by one-way ANOVA followed by Bonferroni's multiple comparison test.

permeabilization and release of apoptogenic molecules from mitochondria to the cytosol (31, 32, 44, 45). The present study indicates that the multidomain proapoptotic Bcl-2 family members Bax and/or Bak play a critical role in regulation of BITC-induced apoptosis. This conclusion is supported by the following observations: (*a*) BITC treatment causes an increase in protein levels of Bax (MCF-7 only) and Bak (MDA-MB-231 and MCF-7), leading to disruption of the mitochondrial membrane potential and cytosolic release of apoptogenic molecules, and (*b*) the SV40-immortalized MEFs derived from Bak-KO and DKO mice are partially yet statistically significantly more resistant toward BITC-induced cell death compared with MEFs derived from WT mice. The BITC-induced apoptosis in MDA-MB-231 cells, but not in MCF-7, may be exacerbated because of down-regulation of Bcl-2 and Bcl-xL. Although further studies are needed to determine the role of Bcl-2 or Bcl-xL in regulation of BITC-mediated cell death in breast cancer cells, it is important to point out that overexpression of Bcl-2 fails to confer significant protection against PEITC-induced apoptosis in PC-3 human prostate cancer cells (26). At the same time, ectopic expression of Bcl-xL protects against PEITC-induced apoptosis in PC-3 cells but only at higher concentrations (46).

Transmission electron microscopy revealed evidence of autophagy in BITC-treated MDA-MB-231 cells without a visible change in mitochondrial morphology, such as swelling (Fig. 8). Autophagy is an evolutionary conserved, dynamic, and lysosome-mediated process for turnover of cellular components, including organelles (47). We have shown recently that D,L-SFN, a synthetic analogue of naturally occurring L-SFN isomer, causes autophagy in PC-3 and LNCaP human prostate cancer cells (48). Autophagic response has also been observed by other cancer-relevant stimuli, including radiation and tumor necrosis factor-α (49, 50). Although the connection between autophagy and apoptotic cell death is not clear, in some systems autophagy seems to promote apoptosis. For example, the formation of autophagosomes is associated with tumor necrosis factor-α–induced apoptosis in human T lymphoblastic leukemia cells (50). On the other hand, autophagy represents a defense mechanism against D,L-SFN-induced apoptosis in human prostate cancer cells by preventing cytosolic release of cytochrome *c* due to sequestration of some mitochondria in autophagosome-like structures (48). It remains to be seen whether BITC-induced autophagy inhibits apoptosis in human breast cancer cells. Likewise, studies are also needed to determine whether BITC-mediated autophagic response is unique to MDA-MB-231 cells.

The BITC-induced apoptosis in our model correlates with ROS production (Fig. 9). The impetus for examining this correlation was provided by a previous study documenting ROS generation by BITC in rat liver epithelial cells (11). Because BITC-mediated ROS generation, cytoplasmic histone-associated DNA fragmentation, and cell killing are significantly attenuated in the presence of a

superoxide dismutase and catalase mimetic (EUK134), it is reasonable to conclude that the cell death caused by BITC in human breast cancer cells is triggered by ROS generation. We have shown previously that ROS generation is a critical event in the initiation of cell death by D,L-SFN (24). However, the precise mechanism of ROS generation by ITCs remains to be elucidated. Because ROS generation is implicated in pathogenesis of many chronic diseases, including cancer, the potential side effects of BITC-mediated ROS production cannot be ignored. Based on the results of the present study and previous findings from our laboratory and by other investigators, we are tempted to speculate that ROS generation by BITC may not be harmful for the following reasons: (*a*) BITC is a dietary agent abundant in many cruciferous vegetables consumed by humans on a daily basis, yet epidemiologic studies continue to support the premise that dietary intake of cruciferous vegetables may reduce the risk of different types of malignancies, including breast cancer (1, 2, 18, 19); (*b*) BITC is relatively safe in animal models (5–10); and (*c*) the MCF-10A normal mammary epithelial cell line

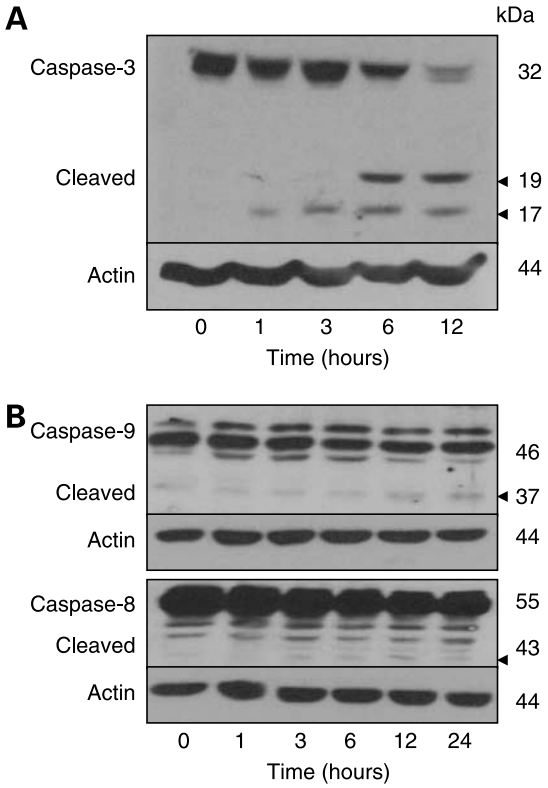

Figure 11. Immunoblotting for cleavage of procaspase-3 (**A**) and procaspase-9 and procaspase-8 (**B**) using lysates from MDA-MB-231 cells exposed to 2.5 μmol/L BITC for the indicated times. The blots were stripped and reprobed with anti-actin antibody as a loading control. Immunoblotting for each protein was done at least twice using independently prepared lysates, and the results were comparable.

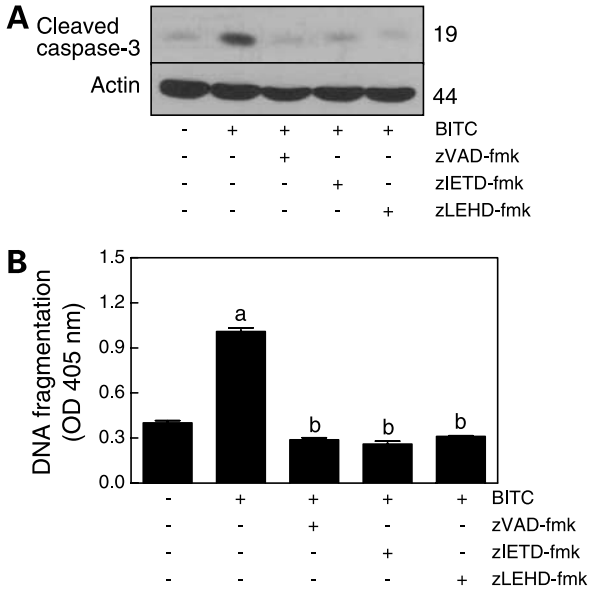

Figure 12. **A,** immunoblotting for cleaved caspase-3 using lysates from MDA-MB-231 cells following treatment with BITC in the presence or absence of pan-caspase inhibitor zVAD-fmk, caspase-9-specific inhibitor zLEHD-fmk, and caspase-8-specific inhibitor zIETD-fmk. The MDA-MB-231 cells were exposed to either DMSO (control) or 40 μmol/L caspase inhibitor for 2 h before BITC treatment (2.5 μmol/L, 24 h). The blot was stripped and reprobed with anti-actin antibody as a loading control. **B,** cytoplasmic histone-associated DNA fragmentation in MDA-MB-231 cells following a 24-h treatment with either DMSO (control) or 2.5 μmol/L BITC in the presence or absence of 40 μmol/L pan-caspase inhibitor zVAD-fmk, caspase-9-specific inhibitor zLEHD-fmk, and caspase-8-specific inhibitor zIETD-fmk. Similar results were observed in two independent experiments. *Columns,* mean ($n = 3$); *bars,* SE. [a], $P < 0.05$, significantly different compared with DMSO-treated control; [b], $P < 0.05$, significantly different compared with BITC alone treatment group by one-way ANOVA followed by Tukey's multiple comparison test.

is resistant to ROS production as well as apoptosis induction by BITC. It is possible that the ROS generation by BITC in cancer cells is transient and serves to trigger the apoptosis signaling cascade.

Apoptosis induction by different stimuli is mediated by activation of caspases, which cause cleavage and inactivation of key cellular proteins (36, 37). The BITC treatment causes cleavage of procaspase-3 that coincides with cleavage of procaspase-9 and procaspase-8 (Fig. 11). Caspase-3 is an executioner caspase that can be activated by a mitochondrial pathway involving caspase-9 or a death receptor pathway involving caspase-8 (36, 37). The results of the present study indicate that BITC-induced apoptosis, at least in MDA-MB-231 cells, is probably mediated by both caspase-9 and caspase-8 because specific inhibitors of these caspases are able to significantly inhibit the cell death caused by BITC.

In conclusion, the results of the present study indicate that BITC inhibits growth of human breast cancer cells in culture by causing G_2-M phase cell cycle arrest and apoptosis, whereas a normal mammary epithelial cell line is somewhat resistant toward these effects. In addition, we provide experimental evidence to implicate

Bak in regulation of BITC-induced apoptosis. These observations provide rationale for further preclinical and clinical evaluation of BITC for its efficacy against breast cancer.

Acknowledgments

We thank Yan Zeng for technical assistance and Dr. Stanley J. Korsmeyer for generous gift of the MEFs.

References

1. Verhoeven DT, Goldbohm RA, van Poppel G, Verhagen H, van den Brandt PA. Epidemiological studies on brassica vegetables and cancer risk. Cancer Epidemiol Biomarkers Prev 1996;5:733 – 48.

2. Cohen JH, Kristal AR, Stanford JL. Fruit and vegetable intakes and prostate cancer risk. J Natl Cancer Inst 2000;92:61 – 8.

3. Conaway CC, Yang YM, Chung FL. Isothiocyanates as cancer chemopreventive agents: their biological activities and metabolism in rodents and humans. Curr Drug Metab 2002;3:233 – 55.

4. Hecht SS. Inhibition of carcinogenesis by isothiocyanates. Drug Metab Rev 2000;32:395 – 411.

5. Wattenberg LW. Inhibition of carcinogenic effects of polycyclic hydrocarbons by benzyl isothiocyanate and related compounds. J Natl Cancer Inst 1977;58:395 – 8.

6. Wattenberg LW. Inhibition of carcinogen-induced neoplasia by sodium cyanate, *tert*-butyl isocyanate, and benzyl isothiocyanate administered subsequent to carcinogen exposure. Cancer Res 1981;41:2991 – 4.

7. Wattenberg LW. Inhibitory effects of benzyl isothiocyanate administered shortly before diethylnitrosamine or benzo[*a*]pyrene on pulmonary and forestomach neoplasia in A/J mice. Carcinogenesis 1987;8:1971 – 3.

8. Lin J, Amin S, Trushin N, Hecht SS. Effects of isothiocyanates on tumorigenesis by benzo[*a*]pyrene in murine tumor models. Cancer Lett 1993;74:151 – 9.

9. Sugie S, Okumura A, Tanaka T, Mori H. Inhibitory effects of benzyl isothiocyanate and benzyl thiocyanate on diethylnitrosamine-induced hepatocarcinogenesis in rats. Jpn J Cancer Res 1993;84:865 – 70.

10. Yang YM, Conaway CC, Chiao JW, et al. Inhibition of benzo(*a*)pyrene-induced lung tumorigenesis in A/J mice by dietary *N*-acetylcysteine conjugates of benzyl and phenethyl isothiocyanates during the postinitiation phase is associated with activation of mitogen-activated protein kinases and p53 activity and induction of apoptosis. Cancer Res 2002;62:2 – 7.

11. Nakamura Y, Kawakami M, Yoshihiro A, et al. Involvement of the mitochondrial death pathway in chemopreventive benzyl isothiocyanate-induced apoptosis. J Biol Chem 2002;277:8492 – 9.

12. Lui VWY, Wentzel AL, Xiao D, Lew KL, Singh SV, Grandis JR. Requirement of a carbon spacer in benzyl isothiocyanate-mediated cytotoxicity and MAPK activation in head and neck squamous cell carcinoma. Carcinogenesis 2003;24:1705 – 12.

13. Srivastava SK, Singh SV. Cell cycle arrest, apoptosis induction and inhibition of nuclear factor κB activation in anti-proliferative activity of benzyl isothiocyanate against human pancreatic cancer cells. Carcinogenesis 2004;25:1701 – 9.

14. Miyoshi N, Uchida K, Osawa T, Nakamura Y. A link between benzyl isothiocyanate-induced cell cycle arrest and apoptosis: involvement of mitogen-activated protein kinases in the Bcl-2 phosphorylation. Cancer Res 2004;64:2134 – 42.

15. Visanji JM, Duthie SJ, Pirie L, Thompson DG, Padfield PJ. Dietary isothiocyanates inhibit Caco-2 cell proliferation and induce G_2/M phase cell cycle arrest, DNA damage, and G_2/M checkpoint activation. J Nutr 2004;134:3121 – 6.

16. Tseng E, Scott-Ramsay EA, Morris ME. Dietary organic isothiocyanates are cytotoxic in human breast cancer MCF-7 and mammary epithelial MCF-12A cell lines. Exp Biol Med (Maywood) 2004;229:835 – 42.

17. Jakubikova J, Sedlak J, Bacon J, Goldson A, Bao Y. Effects of MEK1 and PI3K inhibitors on allyl-, benzyl- and phenylethyl-isothiocyanate-induced G_2/M arrest and cell death in Caco-2 cells. Int J Oncol 2005;27:1449 – 58.

18. Fowke JH, Chung FL, Jin F, et al. Urinary isothiocyanate levels, brassica, and human breast cancer. Cancer Res 2003;63:3980 – 6.

19. Ambrosone CB, McCann SE, Freudenheim JL, Marshall JR, Zhang Y, Shields PG. Breast cancer risk in premenopausal women is inversely associated with consumption of broccoli a source of isothiocyanates, but is not modified by GST genotype. J Nutr 2004;134:1134 – 8.

20. Wei MC, Zong WX, Cheng EH, et al. Proapoptotic Bax and Bak: a requisite gateway to mitochondrial dysfunction and death. Science 2001;292:727 – 30.

21. Xiao D, Choi S, Johnson DE, et al. Diallyl trisulfide-induced apoptosis in human prostate cancer cells involves c-Jun N-terminal kinase and extracellular-signal regulated kinase-mediated phosphorylation of Bcl-2. Oncogene 2004;23:5594 – 606.

22. Xiao D, Zeng Y, Choi S, Lew KL, Nelson JB, Singh SV. Caspase-dependent apoptosis induction by phenethyl isothiocyanate, a cruciferous vegetable-derived cancer chemopreventive agent, is mediated by Bak and Bax. Clin Cancer Res 2005;11:2670 – 9.

23. Singh SV, Herman-Antosiewicz A, Singh AV, et al. Sulforaphane-induced G_2/M phase cell cycle arrest involves checkpoint kinase 2-mediated phosphorylation of Cdc25C. J Biol Chem 2004;279:25813 – 22.

24. Singh SV, Srivastava SK, Choi S, et al. Sulforaphane-induced cell death in human prostate cancer cells is initiated by reactive oxygen species. J Biol Chem 2005;280:19911 – 24.

25. Morse DL, Gray H, Payne CM, Gillies RJ. Docetaxel induces cell death through mitotic catastrophe in human breast cancer cells. Mol Cancer Ther 2005;4:1495 – 504.

26. Xiao D, Johnson CS, Trump DL, Singh SV. Proteasome-mediated degradation of cell division cycle 25C and cyclin-dependent kinase 1 in phenethyl isothiocyanate-induced G_2-M-phase cell cycle arrest in PC-3 human prostate cancer cells. Mol Cancer Ther 2004;3:567 – 75.

27. Xiao D, Herman-Antosiewicz A, Antosiewicz J, et al. Diallyl trisulfide-induced G_2/M phase cell cycle arrest in human prostate cancer cells is caused by reactive oxygen species-dependent destruction and hyperphosphorylation of Cdc25C. Oncogene 2005;24:6256 – 68.

28. Hartwell LH, Kastan MB. Cell cycle control and cancer. Science 1994;266:1821 – 8.

29. Draetta G, Eckstein J. Cdc25 protein phosphatases in cell proliferation. Biochim Biophys Acta 1997;1332:M53 – 63.

30. Hengartner MO. The biochemistry of apoptosis. Nature 2000;407:770 – 6.

31. Chao DT, Korsmeyer SJ. BCL-2 family: regulators of cell death. Annu Rev Immunol 1998;16:395 – 419.

32. Adams JM, Cory S. The Bcl-2 protein family: arbiters of cell survival. Science 1998;281:1322 – 6.

33. Cossarizza A, Baccarani-Contri M, Kalashnikova G, Franceschi C. A new method for the cytofluorimetric analysis of mitochondrial membrane potentials using the J-aggregate forming lipophilic cation 5,5′,6,6′-tetrachloro-1,1′,3,3′-tetraethylbenzimidazolylcarbocyanine iodide (JC-1). Biochem Biophys Res Commun 1993;197:40 – 5.

34. Rothe G, Valet GJ. Flow cytometric analysis of respiratory burst activity in phagocytes with hydroethidine and 2′,7′-dichlorofluorescin. J Leukoc Biol 1990;47:440 – 8.

35. Narayanan PK, Goodwin EH, Lehnert BE. Alpha particles initiate biological production of superoxide anions and hydrogen peroxide in human cells. Cancer Res 1997;57:3963 – 71.

36. Thornberry N, Lazebnick Y. Caspases: enemies within. Science 1998;281:1312 – 6.

37. Wolf BB, Green DR. Suicidal tendencies: apoptotic cell death by caspase family proteinases. J Biol Chem 1999;274:20049 – 52.

38. Liebes L, Conaway CC, Hochster H, et al. High-performance liquid chromatography-based determination of total isothiocyanate levels in human plasma: application to studies with 2-phenethyl isothiocyanate. Anal Biochem 2001;291:279 – 89.

39. Ji Y, Morris ME. Determination of phenethyl isothiocyanate in human plasma and urine by ammonia derivatization and liquid chromatography-tandem mass spectrometry. Anal Biochem 2003;323:39 – 47.

40. Huang C, Ma WY, Li J, Hecht SS, Dong Z. Essential role of p53 in phenethyl isothiocyanate-induced apoptosis. Cancer Res 1998;58:4102 – 6.

41. Agarwal ML, Taylor WR, Chernov MV, Chernova OB, Stark GR. The p53 network. J Biol Chem 1998;273:1 – 4.

42. Sheikh MS, Fornace AJ. Role of p53 family members in apoptosis. J Cell Physiol 2000;182:171 – 81.

43. Taylor WR, Stark GR. Regulation of the G_2/M transition by p53. Oncogene 2001;20:1803 – 15.

44. Reed JC. Bcl-2 family proteins: regulators of apoptosis and chemoresistance in hematologic malignancies. Semin Hematol 1997; 34:9 – 19.

45. Martinou JC, Green DR. Breaking the mitochondrial barrier. Nat Rev Mol Cell Biol 2001;2:63 – 7.

46. Xiao D, Lew KL, Zeng Y, et al. Phenethyl isothiocyanate-induced apoptosis in PC-3 human prostate cancer cells is mediated by reactive oxygen species-dependent disruption of the mitochondrial membrane potential. Carcinogenesis. In press 2006.

47. Ogier-Denis E, Codogno P. Autophagy: a barrier or an adaptive response to cancer. Biochim Biophys Acta 2003;1603:113 – 28.

48. Herman-Antosiewicz A, Johnson DE, Singh SV. Sulforaphane causes autophagy to inhibit release of cytochrome *c* and apoptosis in human prostate cancer cells. Cancer Res 2006;66:5828 – 35.

49. Paglin S, Hollister T, Delohery T, et al. A novel response of cancer cells to radiation involves autophagy and formation of acidic vesicles. Cancer Res 2001;61:439 – 44.

50. Jia L, Dourmashkin RR, Allen PD, Gray AB, Newland AC, Kelsey SM. Inhibition of autophagy abrogates tumour necrosis factor α induced apoptosis in human T-lymphoblastic leukaemic cells. Br J Haematol 1997; 98:673 – 85.

Molecular Cancer Therapeutics

Benzyl isothiocyanate–induced apoptosis in human breast cancer cells is initiated by reactive oxygen species and regulated by Bax and Bak

Dong Xiao, Victor Vogel and Shivendra V. Singh

Mol Cancer Ther 2006;5:2931-2945.